Direct Measurement of the Magnetocaloric Effect through Time-Dependent Magnetometry

R. Almeida,[1] C. Amorim,[2] J. S. Amaral,[2] J. P. Araújo,[1] and J. H. Belo[1,*]

[1]*IFIMUP, Departamento de Física e Astronomia da Faculdade de Ciências da Universidade do Porto, Rua do Campo Alegre, 687, 4169-007 Porto, Portugal*

[2]*Departamento de Física and CICECO, Universidade de Aveiro, 3810-193 Aveiro, Portugal*

(Dated: August 16, 2022)

Abstract

The magnetocaloric effect of a given material is typically assessed through indirect estimates of the isothermal magnetic entropy change, ΔS_M. While estimating the adiabatic temperature difference, ΔT_{ad}, is more relevant from the standpoint of refrigeration device engineering, this requires specialized experimental setups. We here present an approach to directly measure ΔT_{ad} through time-dependent magnetometry in a commercial SQUID device. We use as reference material Gadolinium under a 20 kOe field change, and compare our results with the bibliography. At non-adiabatic experimental conditions, a remarkably similar $\Delta T_{ad}(T)$ curve profile is obtained, however its peak amplitude is underestimated. With a simple compensation methodology we were able to further approximate the profile of the $\Delta T_{ad}(T)$ curve obtaining the peak amplitude, the maximizing temperature, and the FWHM within relative errors of -4%, -0.7%, and 11%, respectively. Our reported approach makes the measurement of both $\Delta S_M(T)$ and $\Delta T_{ad}(T)$ possible with a single instrument, enabling the accelerated progress towards new, competitive, and industry-ready materials.

I. INTRODUCTION

The refrigeration, air-conditioning and heat pumping industry is responsible for nearly 8% of current greenhouse gas emissions [1, 2]. The ever more urgent need to reduce the environmental impact and the restrictions established on the use of gases with high global-warming potential (CFCs, HCFCs, HFCs) have been driving and intensifying the search for potential alternatives to vapor compression technologies [3–5]. One of the most promising candidates is magnetic refrigeration, which completely eliminates the use of these harmful gases and instead uses solid state materials exhibiting a large magnetocaloric effect around room temperature [6–9].

The magnetocaloric effect consists of a magnetic-field induced change of a materials temperature. It is typically quantified by two related quantities: the isothermal magnetic entropy change, ΔS_M, corresponding to the entropy change through the magnetic ordering caused by field application at isothermal conditions, and ΔT_{ad}, the temperature difference upon an adiabatic application of magnetic field. Experimentally, these quantities are most

* jbelo@fc.up.pt

often quantified indirectly by making a set of isothermal (or isofield) magnetization vs. field (or vs. temperature) measurements [10–12], which by using the following Maxwell relation:

$$\left(\frac{\partial S_M\left(H,T\right)}{\partial H}\right)_T = \left(\frac{\partial M\left(H,T\right)}{\partial T}\right)_H \tag{1}$$

can be used to obtain the isothermal entropy change,

$$\Delta S_M(T)_{\Delta H} = \int_{H_i}^{H_f} dS_M(T,H)_T = \int_{H_i}^{H_f} \left(\frac{\partial M(T,H)}{\partial T}\right)_H dH. \tag{2}$$

The adiabatic temperature change can also be measured indirectly through the use of the same Maxwell relation (equation 1) together with calorimetric measurements of the heat capacity vs. temperature and magnetic field, $C_p(T,H)$:

$$\begin{aligned}\Delta T_{ad}\left(T_i\right)_{\Delta H} &= \int_{H_i}^{H_f} dT\left(T_i,H\right)_S = \int_{H_i}^{H_f} \left(\frac{\partial T(T_i,H)}{\partial H}\right)_S dH \\ &= \int_{H_i}^{H_f} -\frac{T_i}{C_p(T_i,H)}\left(\frac{\partial S\left(T_i,H\right)}{\partial H}\right)_T dH \\ &= -\int_{H_i}^{H_f} \frac{T_i}{C_p(T_i,H)\left(\frac{\partial M(T_i,H)}{\partial T}\right)_H dH}\end{aligned} \tag{3}$$

However, this indirect measurement is timely and also implies making a different set of measurements involving calorimetry in order to obtain the temperature and field dependent heat capacity. Measuring the adiabatic temperature change directly - by measuring the temperature change under the application of a magnetic field - also frequently proves inconvenient, due to the difficulty of assuring adiabaticity (i.e. through increased sample size, improved thermal insulation, fast field application and/or a thermocouple of comparatively negligible mass [13–16]). Alternative methods to circumvent these issues, such as non-contact thermometry methods, are still at an early stage and typically demand intricate setups [17–19]. Therefore, an accessible, fast alternative technique to measure the magnetocaloric effect directly is of high interest.

Time-dependent magnetization protocols are usually employed for studying phase transition kinetics (i.e. investigating nucleation and growth, thermal activation processes, etc.) of first-order phase transitions [20–24], which have a more intense magnetocaloric effect than second-order phase transition materials due to a significant magneto-volume coupling [25, 26]. In these, the magnetic field is increased until a certain value (H_{pause}) and thereon

kept constant, while the magnetization is measured as a function of time. However, if employed on a bulky sample within a well thermally-insulated environment, besides phase transformation phenomena, the magnetocaloric effect resulting from the field application will have offset the sample's temperature (by approximately $\Delta T_{ad}(T_{measurement}, H_{pause})$) and a thermal relaxation will follow. This relaxation will be reflected in the sample's magnetization, which will also relax as a function of time. In this paper, we explore the possibility of estimating the temperature variation of a sample following field application (ΔT_{ad}) through fitting the magnetization relaxation as a function of time.

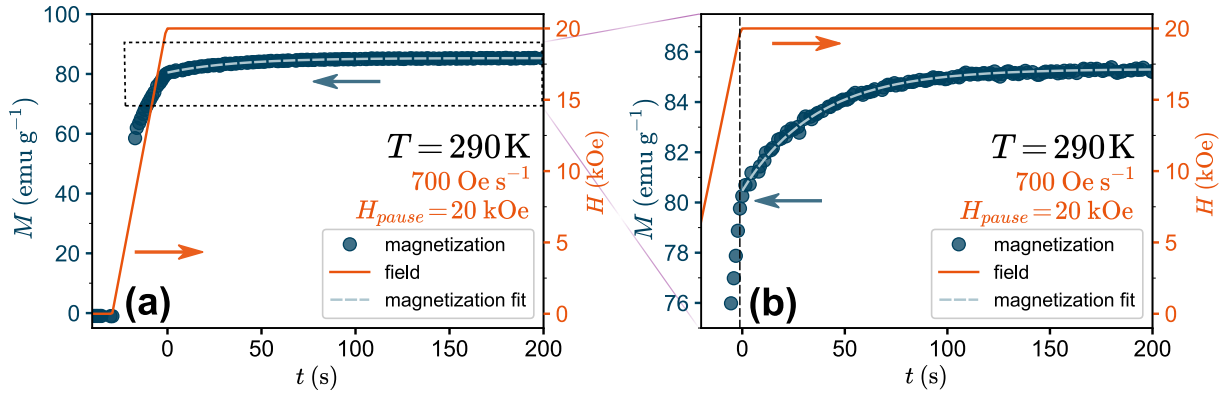

FIG. 1. (a) Schematic of the time-dependent magnetization measurement protocol: a single H_{pause} measurement, showing the magnetization (blue circles assigned to the left y-axis) and field (solid orange line assigned to the right y-axis) versus time. An exponential fit of the form $M_{fit}(t) = m_s - \Delta M e^{-t/\tau}$ is performed to the magnetization relaxation profile for $t > 0$. (b) The same measurement with the relaxation portion ($t > 0$) zoomed in.

The time-dependent magnetization measurement protocol consists of increasing the magnetic field with a constant sweep rate (linearly in time) until a given H_{pause} value is reached, which is then kept constant throughout the rest of the measurement time. The sample's net magnetic moment is continuously measured as a function of time starting from when the magnetic field is still zero through until 300 seconds after the maximum field value, H_{pause}, is reached. In figure 1, both the magnetization and the magnetic field measured for a single run can be seen together with an exponential fit. The time values, t, are all offset so that $t = 0$ coincides with the field reaching its respective maximum value, H_{pause}. The exponential function chosen to fit the observed relaxations is shown in the following equation:

$$M_{fit}(t) = m_s - \Delta M e^{-t/\tau}, \tag{4}$$

where m_s is the converging value of magnetization while approaching thermal equilibrium, ΔM corresponds to the magnitude of relaxation in magnetization from $t = 0$ until thermal equilibrium is reached, and τ corresponds to the characteristic time of the relaxation.

II. EXPERIMENTAL DETAILS

A. Instrumentation

In this work a widely available commercial magnetometer - MPMS-3 SQUID Magnetometer from Quantum Design [27] - was used to measure magnetization as a function of time, while controlling the temperature and magnetic field on the sample. The MPMS-3 can reach a maximum a magnetic field sweep rate of 700 Oe s^{-1} and has a maximum sampling frequency of 1 Hz. The VSM mode was used with a 0.4 mm peak amplitude and an averaging time of 1 s.

B. Sample

In order to test this technique, a polycrystalline, 99.9 % purity (REM) Gd sample with parallelepipedic shape of dimensions $\sim$ 5.5 x 2.5 x 2.5 mm^3 (mounted with its largest spatial dimension along the magnetic field direction) and a mass of 261 mg. Gd presents a second-order phase transition at a Curie temperature of $\sim$ 296 K [28]. Additionally, the same sample was measured in two distinct thermal environments: one regular configuration, with the sample glued to a quartz sample holder with GE varnish, and an insulated configuration, where the sample was wrapped in cotton and teflon tape in addition to being placed inside a gelatin capsule and fixed to a brass sample holder with Kapton tape.

C. Methodology

For estimating the $\Delta T_{ad}(T)$ curve of Gadolinium, we employed a time-dependent protocol for measuring magnetization relaxation in time after applying a 20 kOe field at several differ-

ent background temperatures. During each measurement, the background temperature and thermal conditions are constant, as the temperature difference of the sample is not detected by any of the instruments' thermometers. The magnetization relaxations were subsequently "converted" into relaxations in temperature through a previously obtained magnetization versus temperature curve, also with a 20 kOe field applied. The magnetization was measured as a function of temperature both during heating and during cooling, since despite using a low temperature sweep rate of 1 K min^{-1}, there is still some artificial hysteresis which results from the sample's temperature slightly lagging behind the instrument's measured temperature. This was accounted for by using the average of both curves in the analysis.

III. RESULTS

A. Thermal behaviour

To reinforce the above-mentioned thermal nature of these relaxations, two identical H_{pause} measurements H_{pause} = 20 kOe, at T=290 K and with a 700 Oe s^{-1} field sweep rate) were done on the same sample but using an insulated and a non-insulated thermal setup, as described in section II. If the magnetization relaxation is truly due to the temperature relaxation of our sample, then insulating the sample should slow heat exchange with the environment, resulting in a slower thermal relaxation and thus in a slower relaxation in magnetization. As can be seen in figure 2, the magnetization relaxation was slower for the insulated sample (the fit function yielded a significantly larger characteristic time (τ), in comparison with the non-insulated setup), which is consistent with our interpretation. Additionally, the total magnetization change, ΔM, was also higher for the insulated sample, since it also loses less heat during field application.

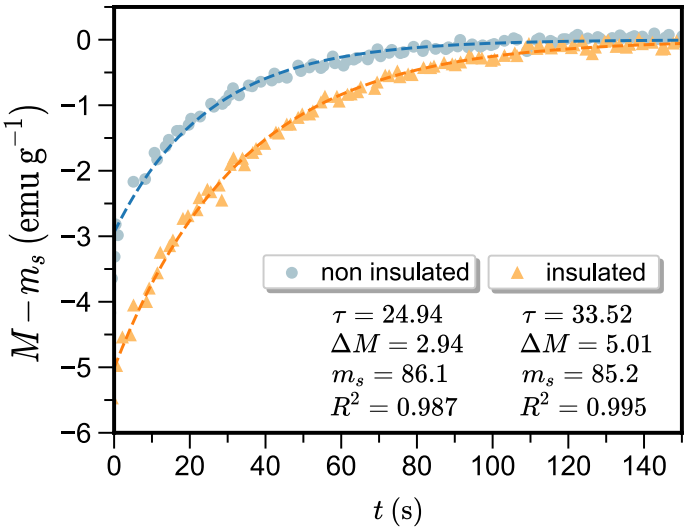

FIG. 2. Two identical (T=290 K and H_{pause}=20 kOe) magnetization versus time measurements were made for the distinct thermal environments of the sample (non-insulated and insulated), where magnetization was subtracted to its equilibrium value (m_s) and time was offset so that $t = 0$ corresponds to the time when the field reached its maximum value (H_{pause}) and stopped changing. The insulated scenario shows a slowing of the relaxation and greater amplitude than the non-insulated one, as is consistent with the thermal interpretation of the phenomena.

This change in magnetization relaxation behaviour strongly supports the thermal interpretation of these relaxation phenomena, which can be understood as follows: as we apply a magnetic field up to H_{pause}, the magnetocaloric effect occurs, i.e. sample temperature increases. The source of the heating can be safely attributed to the magnetocaloric effect alone since it is much more significant than any heat generated from induction, according to theoretical calculations and previous experimental data [14, 29]. Then, thermal relaxation will occur as the sample releases heat to its surroundings and decreases its temperature down to the initial measurement temperature ($T_{measurement}$). Since the sample temperature influences (drastically near T_c) the sample's magnetization, then this thermal relaxation will manifest itself on a simultaneous magnetization relaxation. When the field is constant (after H_{pause} is reached), the sample's magnetization will in principle follow the same temperature dependence as obtained through an isofield temperature sweep with the same field, $M(T, H = H_{pause})$ applied. Such a $M(T, H = H_{pause})$ curve can then be used to convert the magnetization values from the relaxation to temperature, effectively using the magnetization

as an intrinsic thermometer. This idea is schematically pictured in figure 3.

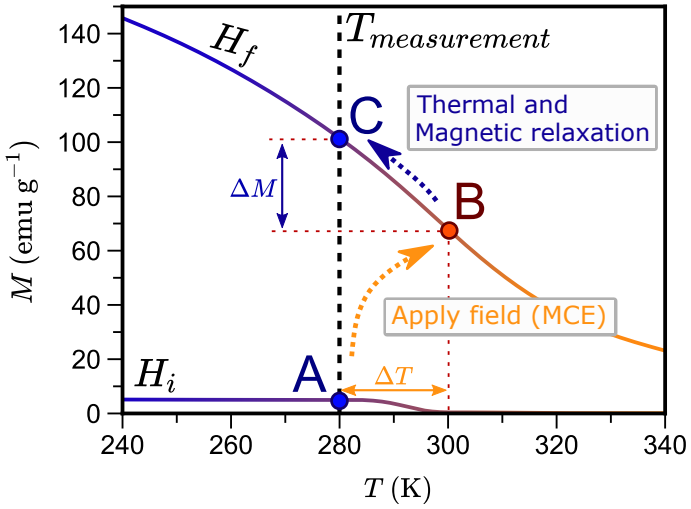

FIG. 3. A schematic of the thermal interpretation of the magnetization relaxation behaviour. The two curves correspond to equilibrium measurements of the magnetization versus temperatures at two different magnetic fields ($H_i \ll H_f$). Applying a magnetic field rapidly (A $\rightarrow$ B) results in a non-isothermal increase of magnetization (orange dotted arrow), as it is accompanied by the heating of the sample induced by the magnetocaloric effect. The resultant thermal relaxation (B $\rightarrow$ C) is reflected in a relaxation of magnetization (blue dashed arrow).

B. Estimating ΔT_{ad} from time-dependent magnetization data

To extract thermal information from the magnetization relaxation data, we assumed an ideal lumped-capacitance temperature relaxation model (valid for a homogenous temperature profile within a sample), i.e. an exponential temperature variation with time:

$$T(t) = \Delta T e^{-t/\tau} + T_{eq}. \tag{5}$$

The magnetization relaxations in time are subsequently modelled simply through the compound function of the isofield magnetization versus temperature and the temperature relaxation curves: $M(T(t), H = H_{pause})$. On the top side of figure 4, examples of simulated $M(T(t), H = H_{pause})$ curves are provided by considering different amplitudes ΔT of the thermal relaxation curve, $T(t)$, and an illustrative characteristic time of 50 s.

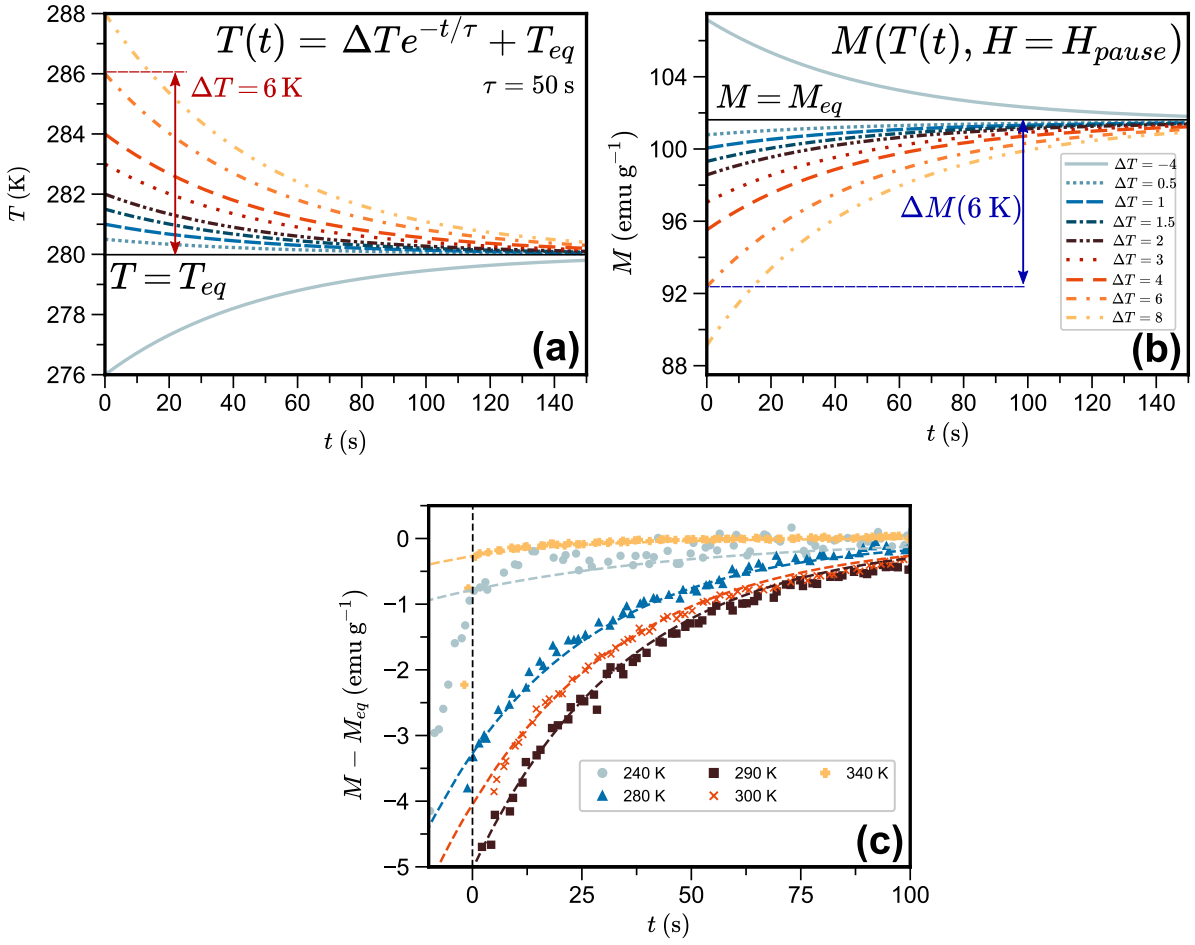

FIG. 4. Modelling and fitting relaxations in temperature and magnetization: considering **(a)** ideal exponential curves as models for the thermal relaxation of our sample, we can take the compound function $M(T(t), H = H_{pause})$ of an experimentally obtained $M(T, H = H_{pause})$ curve (see figure 3) to numerically obtain **(b)** magnetization relaxations in time. The ΔT and ΔM parameters are indicated for the $\Delta T = 6$ K curve; **(c)** A representative set of the time-dependent magnetization measurements for the Gadolinium sample with $H_{pause} = 20$ kOe at different measurement temperatures, $T_{measurement}$, and their respective fits (dashed lines). The equilibrium magnetization ($M_{eq} = m_s$) was subtracted from the magnetization values, allowing for better comparison of the amplitudes at different temperatures.

These numerically obtained curves can then be used in numerical fits to obtain the parameters of our temperature exponential, namely ΔT, which will quantify the amplitude of

the temperature difference during the relaxation after field application, i.e. the adiabatic temperature change (ΔT_{ad}).

To employ this approach on our insulated Gadolinium sample, we used the time-dependent magnetometry protocol measurements with $H_{pause} = 20$ kOe described previously for a set of different measuring temperatures, $T_{measurement}$, around Gadolinium's T_C (296 K). Five representative measurements are displayed on the bottom side of figure 4. The relaxation amplitudes clearly have a peak near 290 K, falling down as the temperature moves away from this value, which is precisely the behaviour of the adiabatic temperature change. This correlation is further evidence of the thermal nature of these relaxations.

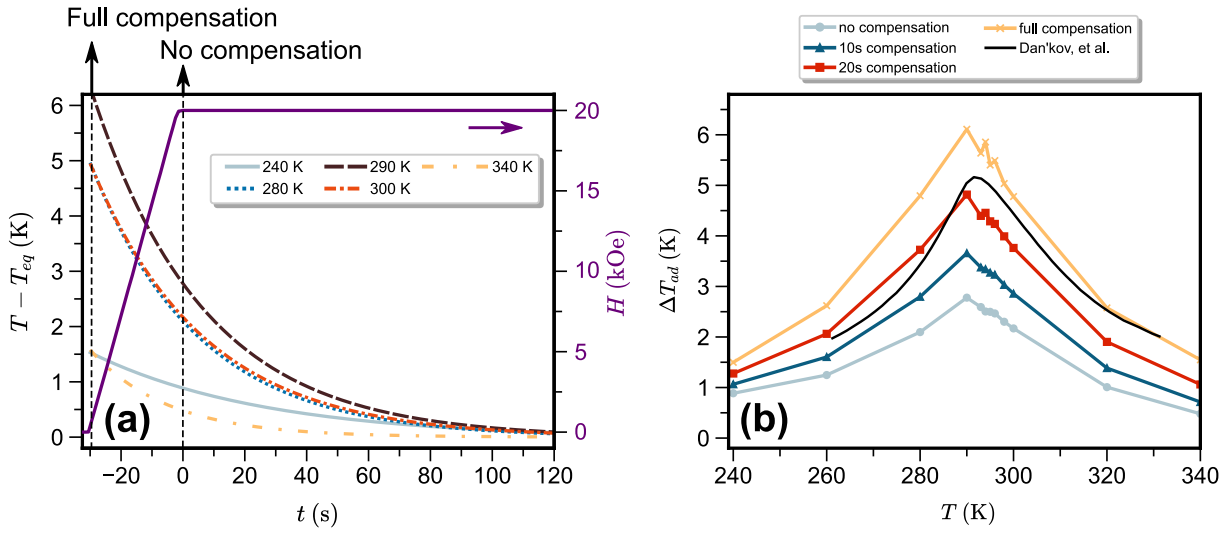

FIG. 5. **(a)** The backwards-extrapolated temperature exponentials obtained from the fits, and **(b)** the estimations of the magnetocaloric effect of Gadolinium for a 20 kOe applied field at different temperatures, for different compensations of the time that it took to apply the field to values, as compared to values from the literature [28].

By performing the above-mentioned numerical fits to each H_{pause} magnetization relaxation measurement, the parameters of the exponential in temperature, τ, ΔT and $T_{measurement}$, were obtained for each temperature.

We have thus estimated the amplitude of the temperature increase of our sample with a 20 kOe field at different starting temperatures. The resultant ΔT_{ad} vs. temperature curve for $H_{pause} = 20$ kOe is shown in figure 6 b) (the "no compensation curve" in light blue dots). Although this curve presents a similar profile as that of the literature (black line)

[28], it clearly underestimates the effect, as can be seen by the temperature offset between the two curves. Such underestimation can be explained due to the fact that while the field is being ramped up, the sample is already exchanging heat with its surroundings, as implied by the changes observed by insulating the sample thermally (figure 2). Even though we have reduced this effect by insulating our sample, it takes about 28 seconds for the field to reach the maximum value of 20 kOe. Considering the time constant of the relaxations (figure 2), this is a very significant time window during which heat is lost, thus compromising the adiabaticity requirement of the field application. If the thermal relaxation is approximately exponential, then the lack of adiabatic conditions will result in a significant underestimation of the adiabatic temperature change (the amplitude of the magnetocaloric effect) for our sample. So, in order to improve the estimation of the ΔT_{ad}, a simple compensation technique was implemented: we extrapolated the temperature function $T(t)$ obtained through our numerical fits of $M(T(t))$ back in time. Since it would be difficult to know the ideal compensation time, we chose a small set of time windows representing different degrees of compensation: 0 seconds (no compensation, corresponding to the temperature difference at $t = 0$), 10 seconds, 20 seconds, and about 28 seconds (full compensation of the time it took to apply the field).

In figure 5, our estimations of ΔT_{ad} for different compensations of the time that it took to apply the field are compared to values from the literature for Gadolinium [28]. As expected, making no compensation results in a significant (-44%) underestimation of ΔT_{ad}. The full compensation achieves a reduced relative error ($+24\%$). The scenario of compensating for the complete time of field application assumes that the field is instantly applied and the thermal relaxation is ongoing from that moment on. This is not accurate, since the field is continuously increased throughout this time, so it is expected that the full compensation overestimates the adiabatic temperature difference. Out of the shown curves, the best results were obtained through compensating for 20 seconds of the field application time, achieving a relative error on the maximum intensity of -4%, which is lower than that obtained through conventional direct measurement methods [28]. The maximizing temperature and the FWHM of this curve were -0.7% and $+11\%$, respectively, as compared to the reference values in [28].

IV. CONCLUSIONS

In this work, a methodology to measure ΔT_{ad} via time-dependent magnetometry is presented and applied to Gadolinium under a 20 kOe field change, using a commercial Quantum Design MPMS3 SQUID magnetometer. With a field sweeping rate of 700 Oe s^{-1}, a 20 kOe field is only reached after 28 s. As the sample is under non-adiabatic conditions, a direct estimate of ΔT_{ad} without correcting for heat exchange during field sweeping leads to an underestimation of the amplitude of the temperature difference as compared to previously published values. In order to correct for this, a simple compensation technique of extrapolating the obtained thermal relaxation exponentials back to the beginning of the field gave better results, albeit overestimated. By considering an intermediate value of time compensation, a final $\Delta T_{ad}(T)$ estimate led to remarkably low deviations of -4% of the peak value, -0.7% of the maximizing temperature and 11% of the FWHM relative to the reference.

The quality of these results should be considered along with the caveat that estimating the most reasonable percentage of compensation would require detailed information about the thermal environment of the sample within the instrument. Our method will give the user a window of possible ranges for the value of $\Delta T_{ad}(T)$: it is certainly over the value obtained without compensation (since the sample loses heat during field application), and certainly under the value of full compensation (since the sample does not heat up instantly when the field starts ramping, but instead heats up throughout the ramping time). In this work, compensating for about 70 % of the field application time (20 s) yielded a good approximation of the real $\Delta T_{ad}(T)$ values, however, this amount may differ for other samples and experimental setups. Getting reliable results while avoiding the need for the knowledge of what the best compensation time is can be accomplished by minimizing the need for any significant compensation. This can be achieved by increasing significantly the field application rate and/or greatly improving the thermal insulation of the sample.

This methodology was herein employed on Gd, the benchmark second-order phase transition material [30]. Metastability would make it harder to apply in first-order phase transition materials, as the magnetization is not only a function of temperature and field but also of the history of the material, so obtaining the correct $M(T)$ curve to use in the numerical fits would be a challenge. Despite this, the simplicity and accessibility of this approach, which allows the estimation of both ΔT_{ad} and ΔS_M with a single instrument for second order ma-

terials, makes it very interesting for the entire multi-caloric materials research community.

ACKNOWLEDGMENTS

This work was developed within the scope of the following projects financed by EEA grants via the project FBR_OC1_85 and by the Portuguese national funding agency for science, research and technology (FCT): UIDB/50011/2020 and UIDP/50011/2020 (CICECO), and PTDC/EME-TED/3099/2020 (IFIMUP). J. H. Belo also thanks FCT for the projects PTDC/FISMAC/31302/2017 and CERN/FISTEC/0003/2019 and for his contract DL57/2016 reference SFRH-BPD-87430/2012.

[1] United Nations Environment Programme, Briefing Note A - The Importance of Energy Efficiency in the Refrigeration, Air-conditioning and Heat Pump Sectors (2018).

[2] J. L. Dupont, P. Domanski, P. Lebrun, and F. Ziegler, The role of refrigeration in the global economy, 38th note on refrigeration technologies, International Institute of Refrigeration (2019).

[3] N. Terada and H. Mamiya, High-efficiency magnetic refrigeration using holmium, Nat. Commun. **12**, 1212 (2021).

[4] European Parliament, The COP26 Climate Change Conference - Status of climate negotiations and issues at stake (2021).

[5] S. Tassou, J. Lewis, Y. Ge, A. Hadawey, and I. Chaer, A review of emerging technologies for food refrigeration applications, Appl. Therm. Eng. **30**, 263 (2010).

[6] V. Franco, J. Blázquez, J. Ipus, J. Law, L. Moreno-Ramírez, and A. Conde, Magnetocaloric effect: From materials research to refrigeration devices, Prog. Mater. Sci. **93**, 112 (2018).

[7] O. Gutfleisch, M. A. Willard, E. Brück, C. H. Chen, S. G. Sankar, and J. P. Liu, Magnetic materials and devices for the 21st century: Stronger, lighter, and more energy efficient, Adv. Mater. **23**, 821 (2010).

[8] A. Kitanovski, Energy applications of magnetocaloric materials, Adv. Energy Mater. **10**, 1903741 (2020).

[9] T. Gottschall, K. P. Skokov, M. Fries, A. Taubel, I. Radulov, F. Scheibel, D. Benke, S. Riegg,

and O. Gutfleisch, Making a cool choice: The materials library of magnetic refrigeration, Adv. Energy Mater. **9**, 1901322 (2019).

[10] V. Franco, J. Blázquez, J. Ipus, J. Law, L. Moreno-Ramírez, and A. Conde, Magnetocaloric effect: From materials research to refrigeration devices, Prog. Mater. Sci. **93**, 112 (2018).

[11] J. Amaral and V. Amaral, On estimating the magnetocaloric effect from magnetization measurements, J. Magn. Magn. Mater. **322**, 1552 (2010).

[12] V. K. Pecharsky and K. A. Gschneidner, Magnetocaloric effect from indirect measurements: Magnetization and heat capacity, J. Appl. Phys. **86**, 565 (1999).

[13] F. Cugini and M. Solzi, On the direct measurement of the adiabatic temperature change of magnetocaloric materials, Journal of Applied Physics **127**, 123901 (2020).

[14] T. Gottschall, M. D. Kuz'min, K. P. Skokov, Y. Skourski, M. Fries, O. Gutfleisch, M. G. Zavareh, D. L. Schlagel, Y. Mudryk, V. Pecharsky, and J. Wosnitza, Magnetocaloric effect of gadolinium in high magnetic fields, Phys. Rev. B **99**, 134429 (2019).

[15] B. R. Gopal, R. Chahine, and T. K. Bose, A sample translatory type insert for automated magnetocaloric effect measurements, Rev. Sci. Instrum. **68**, 1818 (1997).

[16] M. G. Zavareh, Y. Skourski, K. Skokov, D. Karpenkov, L. Zvyagina, A. Waske, D. Haskel, M. Zhernenkov, J. Wosnitza, and O. Gutfleisch, Direct measurement of the magnetocaloric effect in La(Fe, Si, Co)13 compounds in pulsed magnetic fields, Phys. Rev. Appl. **8**, 014037 (2017).

[17] Y. Koshkid'ko, J. Ćwik, T. Ivanova, S. Nikitin, M. Miller, and K. Rogacki, Magnetocaloric properties of gd in fields up to 14 t, J. Magn. Magn. Mater. **433**, 234 (2017).

[18] J. Y. Law, V. Franco, and R. V. Ramanujan, Direct magnetocaloric measurements of Fe-B-Cr-X (X = La, Ce) amorphous ribbons, J. Appl. Phys. **110**, 023907 (2011).

[19] F. Cugini, G. Porcari, C. Viappiani, L. Caron, A. O. dos Santos, L. P. Cardoso, E. C. Passamani, J. R. C. Proveti, S. Gama, E. Brück, and M. Solzi, Millisecond direct measurement of the magnetocaloric effect of a Fe2P-based compound by the mirage effect, Appl. Phys. Lett. **108**, 012407 (2016).

[20] D. Jang, T. Gruner, A. Steppke, K. Mitsumoto, C. Geibel, and M. Brando, Large magnetocaloric effect and adiabatic demagnetization refrigeration with YbPt2Sn, Nat. Commun. **6**, 1 (2015).

[21] V. Basso, M. Piazzi, C. Bennati, and C. Curcio, Hysteresis and phase transition kinetics in

magnetocaloric materials, Phys. Status Solidi (b) **255**, 1700278 (2017).

[22] E. Lovell, A. M. Pereira, A. D. Caplin, J. Lyubina, and L. F. Cohen, Dynamics of the First-Order Metamagnetic Transition in Magnetocaloric La(Fe, Si) 13: Reducing Hysteresis, Advanced Energy Materials **5**, 1401639 (2015).

[23] M. K. Chattopadhyay, M. A. Manekar, A. O. Pecharsky, V. K. Pecharsky, K. A. Gschneidner, J. Moore, G. K. Perkins, Y. V. Bugoslavsky, S. B. Roy, P. Chaddah, and L. F. Cohen, Metastable magnetic response across the antiferromagnetic to ferromagnetic transition in Gd5Ge4, Phys. Rev. B **70**, 21 (2004).

[24] J. Leib, J. E. Snyder, T. A. Lograsso, D. Schlagel, and D. C. Jiles, Dynamics of the magnetic field-induced first order magnetic-structural phase transformation of Gd5(Si0.5Ge0.5)4, J. Appl. Phys. **95**, 6915 (2004).

[25] A. M. Pereira, E. Kampert, J. M. Moreira, U. Zeitler, J. H. Belo, C. Magen, P. A. Algarabel, L. Morellon, M. R. Ibarra, J. N. Gonçalves, J. S. Amaral, V. S. Amaral, J. B. Sousa, and J. P. Araújo, Unveiling the (De)coupling of magnetostructural transition nature in magnetocaloric R5Si2Ge2 (R = Tb, Gd) materials, Appl. Phys. Lett. **99**, 132510 (2011).

[26] N. Marcano, P. A. Algarabel, L. F. Barquín, J. P. Araujo, A. M. Pereira, J. H. Belo, C. Magén, L. Morellón, and M. R. Ibarra, Cluster-glass dynamics of the Griffiths phase in Tb5-xLaxSi2Ge2, Phys. Rev. B **99**, 054419 (2019).

[27] Quantum Design North America, SQUID Magnetometer - Quantum Design MPMS 3 .

[28] S. Y. Dan'kov, A. M. Tishin, V. K. Pecharsky, and K. A. Gschneidner, Magnetic phase transitions and the magnetothermal properties of gadolinium, Phys. Rev. B **57**, 3478 (1998).

[29] E. J. Davies, Conduction and Induction Heating, Institution of Engineering and Technology (1990).

[30] J. Y. Law, V. Franco, L. M. Moreno-Ramírez, A. Conde, D. Y. Karpenkov, I. Radulov, K. P. Skokov, and O. Gutfleisch, A quantitative criterion for determining the order of magnetic phase transitions using the magnetocaloric effect, Nat. Commun. **9**, 2680 (2018).